Nonseparable 2-D FIR filter design using nonuniform frequency sampling

Sonali Bagchi Sanjit K. Mitra
Department of Electrical and Computer Engineering
Signal and Image Processing Laboratory
University of California
Santa Barbara, California 93106

ABSTRACT

We propose a nonuniform frequency sampling method for 2-D FIR filter design based on the concept of the nonuniform discrete Fourier transform (NDFT). The NDFT of a 2-D sequence is defined as a sequence of samples of its z-transform taken at distinct points located arbitrarily in the (z_1, z_2) space. In our design method, we determine the independent filter coefficients by taking samples of the desired frequency response at points located nonuniformly on the unit bi-disc, and then solving the linear equations given by the NDFT formulation. The choice of sample values and locations depends on the shape of the 2-D filter. Best results are obtained when samples are placed on contour lines that match the desired passband shape. The proposed method produces nonseparable filters with good passband shapes and low peak ripples. In this paper, we consider the design of square-and diamond-shaped filters. Extensive comparisons with filters designed by other methods demonstrate the effectiveness of the proposed method. We also investigate the performances of the filters designed by applying them as prefilters and postfilters to schemes for rectangular and quincunx downsampling of images. Examples show that the filters designed by our method produce output images which are sharper and have a higher PSNR, as compared with other filters.

Keywords: 2-D FIR filter design, NDFT, nonuniform frequency sampling, square-and diamond-shaped 2-D filters.

1 INTRODUCTION

We apply the concept of the *nonuniform discrete Fourier transform* (NDFT) to design 2-D FIR filters by nonuniform frequency sampling. As proposed in [1], the NDFT of a 2-D sequence $x[n_1, n_2]$ of size $N_1 \times N_2$ is defined as a sequence of samples of its 2-D z-transform $X(z_1, z_2)$, taken at $N_1 N_2$ distinct points located arbitrarily in the 4-D (z_1, z_2) space. These points can be chosen arbitrarily but in such a way that the inverse transform exists [1]. Therefore, nonuniform sampling on the unit bi-disc corresponds to the case: $z_1 = e^{j\omega_1}$, $z_1 = e^{j\omega_1}$. Earlier efforts in nonuniform 2-D frequency sampling design have involved either constrained sampling structures which reduce computational complexity [2–5], or a linear least squares approach that guarantees unique interpolation [5]. Our approach involves generalized frequency sampling, where the samples are placed on contour lines that match the desired shape of the passband or stopband of the 2-D filter. The proposed method produces nonseparable 2-D filters with good passband shapes and low peak ripple. Filters of good quality are obtained, even with small regions of support. This is important since such filters are most likely to be used in practical

 0-8194-1768-8/95/$6.00

filtering applications.

This paper is organized as follows. The general strategy for the proposed 2-D nonuniform frequency sampling filter design method is outlined in Section 2. Details of the procedure for designing 2-D filters with square-and diamond-shaped passbands are given in Sections 3 and 4, respectively. We also present filter design examples and comparisons with filters obtained by other design methods. In Section 5, we apply the filters designed, as prefilters and postfilters to schemes for rectangular and quincunx downsampling of images. Section 6 contains the concluding remarks.

2 PROPOSED 2-D NONUNIFORM FREQUENCY SAMPLING DESIGN

In the proposed 2-D filter design method, the desired frequency response is sampled at N_i points located nonuniformly in the 2-D frequency plane, where N_i is the number of independent filter coefficients. All symmetries present in the filter impulse response are utilized so that N_i is typically much lower than the total number of filter coefficients, N^2. This reduces the design time, besides guaranteeing symmetry. The set of N_i linear equations given by the 2-D NDFT formulation [1] is then solved to obtain the filter coefficients.

As in the case of 1-D filter design [6], the choice of the sample values and locations depends on the particular type of filter being designed. In general, the problem of locating the 2-D frequency samples is much more complex than in the 1-D case. Our experience in designing 2-D filters with various shapes indicates that best results are obtained when the samples are placed on *contour lines* that match the desired passband shape. For example, to design a square-shaped filter, we place the samples along a set of square contour lines in the 2-D frequency plane. Note that these results agree with the filter design results in [4] and [5], where better control over shape was obtained by placing samples at the edges of the passband and the stopband. The total number of contours and number of samples on each contour have to be chosen carefully so as to avoid singularities. A necessary condition for nonsingularity is known [5, Theorem 2, p. 171] and helps to serve as a rough check. However, this condition is not sufficient to guarantee nonsingularity. The theorem asserts that if the sum of the degrees of the irreducible curves, on which the samples are placed, is small compared to the degree of the filter polynomial, then the interpolation problem becomes singular. Going back to our example of designing a square filter, it is clear that the number of square contours must be chosen appropriately with respect to the filter size.

As we locate the frequency samples along contour lines of the desired shape, the *parameters* to be chosen are: (a) the number of contours and the spacing between them, (b) the number of samples on each contour and their relative spacing, and (c) the sample values. In the following sections, we show how these parameters are chosen for square-and diamond-shaped filters. A common approach used is that a particular *cross-section* of the desired 2-D frequency response is approximated by 1-D analytic functions based on Chebyshev polynomials, similar to those used for 1-D FIR filter design in [6,7]. The samples are then placed on contours that pass through the extrema of this cross-section. This will become clear when we look at design examples in the following sections.

3 SQUARE FILTER DESIGN

Consider the design of a square-shaped lowpass filter $h[n_1, n_2]$, whose frequency-response specification is shown in Figure 1. Let the filter be of size $N \times N$, with passband edge ω_p and stopband edge ω_s, as defined in Figure 1. Since the frequency response exhibits a fourfold symmetry, the zero-phase response $H(\omega_1, \omega_2)$ can be expressed

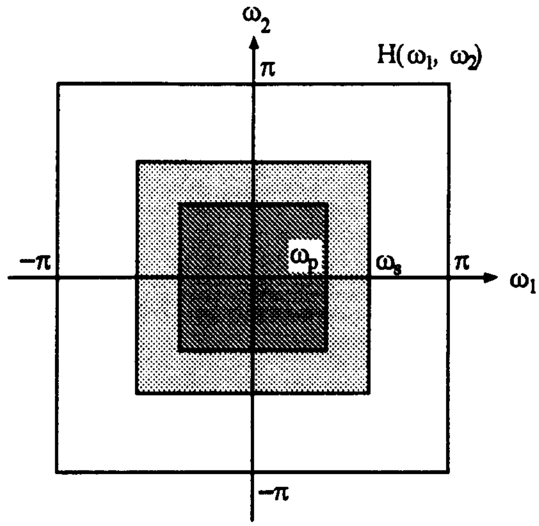

Figure 1: Frequency-response specification of a square-shaped lowpass filter. Shaded region: passband, dotted region: transition band, unshaded region: stopband.

in the form [8]

$$H(\omega_1,\omega_2) = h[0,0] + \sum_{n_1=1}^{(N-1)/2} 2h[n_1,0]\cos\omega_1 n_1 + \sum_{n_2=1}^{(N-1)/2} 2h[0,n_2]\cos\omega_2 n_2 + \sum_{n_1=1}^{(N-1)/2}\sum_{n_2=1}^{(N-1)/2} 4h[n_1,n_2]\cos\omega_1 n_1\cos\omega_2 n_2. \quad (1)$$

Thus, the number of independent filter coefficients is $N_i = (N+1)^2/4$. To solve for these coefficients, we require N_i samples of $H(\omega_1,\omega_2)$ located in the first quadrant of the (ω_1,ω_2) plane.

Our design method is based on the following idea. If we take a cross-section of the 2-D frequency response along the ω_1 axis (or ω_2 axis), then the plot looks like a 1-D lowpass filter response. An example of this cross-section is shown in Figure 2. Given the 2-D filter specifications such as the support size and band-edges, we first represent the passband and stopband of this cross-section by separate analytic functions, $H_p(\omega)$ and $H_s(\omega)$, as done earlier for 1-D lowpass filter design [7]. Then we place samples along the ω_1 axis, at the extrema of these functions [6]. In the 2-D frequency plane, the samples are placed on squares passing through these extrema. All the samples on a particular square have the same value and are evenly spaced. The total number of square contours is $(N+1)/2$. The number of samples on the kth contour starting from the origin is $(2k-1)$, for $k = 1, 2, \ldots, (N+1)/2$. This choice works well, since the total number of samples is given by the sum of the series of $(N+1)/2$ odd numbers:

$$\sum_{k=1}^{(N+1)/2} (2k-1) = \left(\frac{N+1}{2}\right)^2, \quad (2)$$

which equals N_i.

The filter coefficients are found by solving the N_i equations obtained by sampling Eq. (1) at N_i points. The above design method can also be used to design square-shaped ***highpass*** filters. In this case, only one modification is required—the cross-section of the 2-D frequency response along the ω_1 axis (or ω_2 axis) has to be approximated by a 1-D highpass response. The following example illustrates the design method.

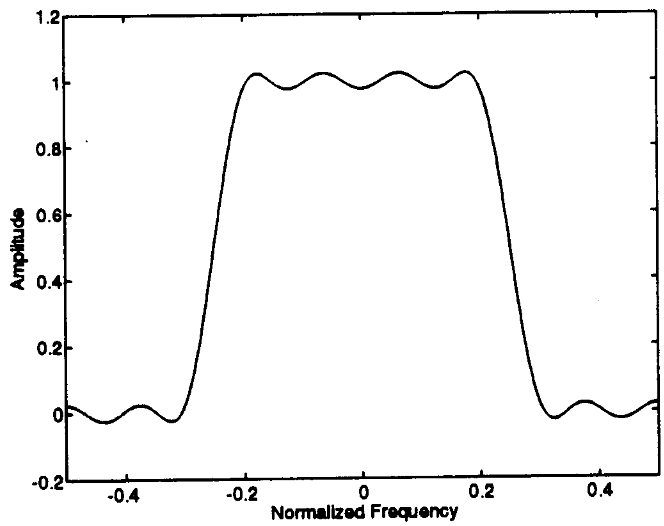

Figure 2: Cross-section of desired square filter frequency response along the ω_1 axis.

Example 1. Consider the design of a square lowpass filter with the specifications: support size $= 9 \times 9$, $\omega_p = 0.35\pi$, $\omega_s = 0.65\pi$. Since only 25 of the 81 filter coefficients are independent, we require 25 samples located in the first quadrant of the 2-D frequency plane. The total number of square contours is five. The cross-section of the 2-D frequency response along the ω_1 axis is represented by 1-D analytic functions, as shown in Figure 3. Then, the location and values of the five samples along the ω_1 axis are obtained by sampling these functions, as marked by "$*$" in Figure 3. Finally, the remaining samples are placed on five successive squares passing through these points, as illustrated on the contour plot in Figure 4(a). The frequency response is also shown in this figure. Clearly, the passband has the desired square shape.

The frequency response of a square filter, shown in Fig. 1, is essentially a separable one. We can design a separable 2-D square filter $h[n_1, n_2]$ by first designing two 1-D lowpass filters $h_1[n]$ and $h_2[n]$, and then simply taking their product along orthogonal directions. Separable filters are widely used in practice because of their design simplicity and ease of implementation. However, they suffer from the following problem. If δ_{p_1}, δ_{s_1} and δ_{p_2}, δ_{s_2} are the peak ripples in the passband and stopband of the two 1-D filters, respectively, then the resulting 2-D filter can have peak ripples as large as $(\delta_{p_1} + \delta_{p_2})$ in the passband, and $\max(\delta_{s_1}, \delta_{s_2})$ in the stopband. Thus, the 2-D filter might have large passband ripple, which is undesirable. In such cases, much better results can be obtained by utilizing the N^2 degrees of freedom available in designing a nonseparable filter, instead of the $2N$ degrees used in a separable design.

We now compare the nonseparable square filter in Example 1 to a separable filter, designed with the same specifications. The Parks-McClellan algorithm is used to design the corresponding 1-D lowpass filter with length $N = 9$, and band-edges as specified in Example 1. Figure 4(b) shows the frequency response and contour plot of the separable square filter. Note the large ripple obtained in the passband. The comparative performance is shown in Table 1. We denote the peak ripples obtained in the passband and stopband by δ_p and δ_s, respectively. Note that the peak passband ripple obtained by our method is nearly a third of that present in the separable filter.

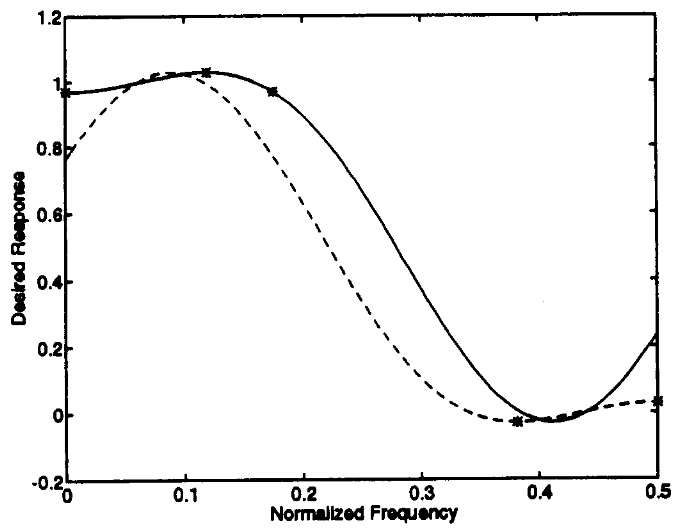

Figure 3: Generation of analytic functions for square filter designed by the NDFT method. The cross-section of the 2-D frequency response along the ω_1 axis is approximated by $H_p(\omega)$ (solid line) in the passband, and $H_s(\omega)$ (dashed line) in the stopband. These functions are sampled at the locations denoted by "*".

Table 1: Comparative performance for square filter design.

Method	δ_p	δ_s
NDFT	0.0322	0.0471
Separable Design	0.1116	0.0579

4 DIAMOND FILTER DESIGN

Diamond filters find important practical applications as prefilters for quincunxially sampled data, and in interlaced-to-noninterlaced scanning converters for television signals. A diamond filter has a frequency-response specification with passband edge ω_p and stopband edge ω_s, as defined in Figure 5. In other words, the diagonal line $\omega_1 = \omega_2$ in the frequency plane intersects the passband edge at (ω_p, ω_p) and the stopband edge at (ω_s, ω_s). A diamond filter exhibits an eightfold symmetry in the frequency domain [8]. Besides, a diamond filter is a 2-D half-band filter. Its frequency response $H(\omega_1, \omega_2)$ is symmetric about the point $(\omega_1, \omega_2, H) = (\pi/2, \pi/2, 0.5)$ in frequency space. This implies that the impulse response has alternating zeros, as given by

$$h[n_1, n_2] = \begin{cases} 0, & n_1 + n_2 = \text{even}, \\ 0.5, & n_1 = n_2 = 0. \end{cases} \qquad (3)$$

On account of these symmetries, the number of independent coefficients [9] in a filter of size $N \times N$ is reduced to

$$N_i = \left\lfloor \frac{P+1}{2} \right\rfloor \left\lfloor \frac{P+2}{2} \right\rfloor, \qquad (4)$$

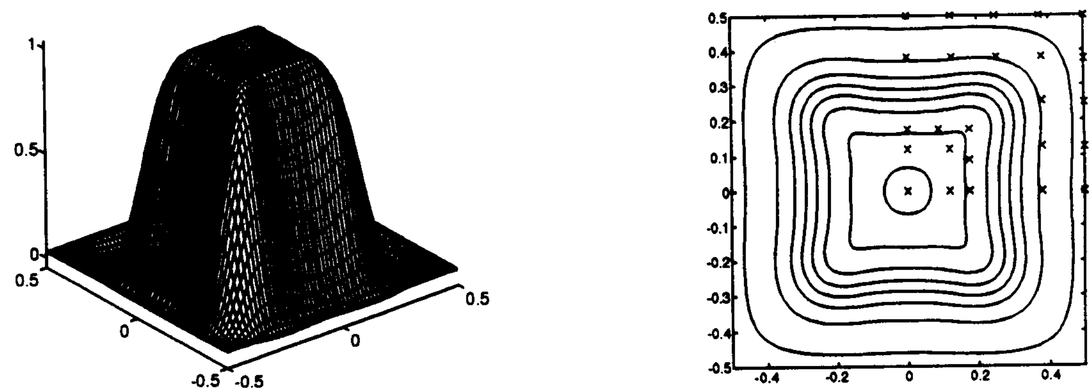

(a)

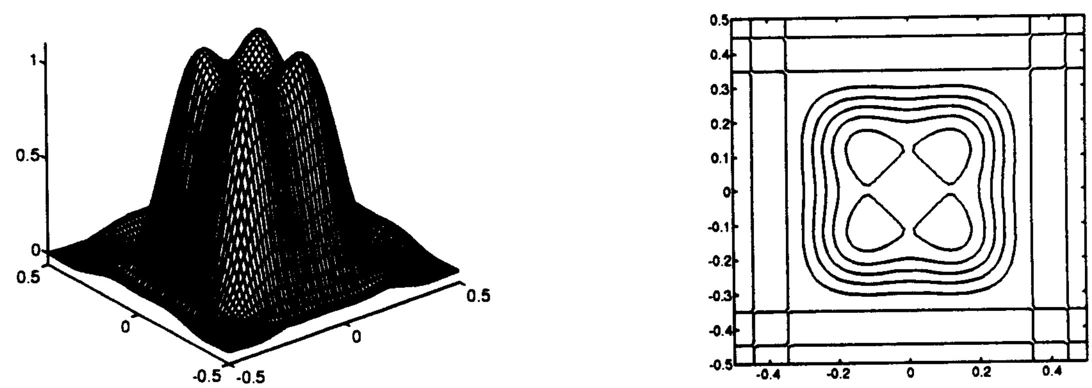

(b)

Figure 4: Frequency response and contour plot for square filters of size 9×9 designed by (a) NDFT method, and (b) separable design method. The sample locations for the NDFT method are denoted by "$\times$" on the corresponding contour plot.

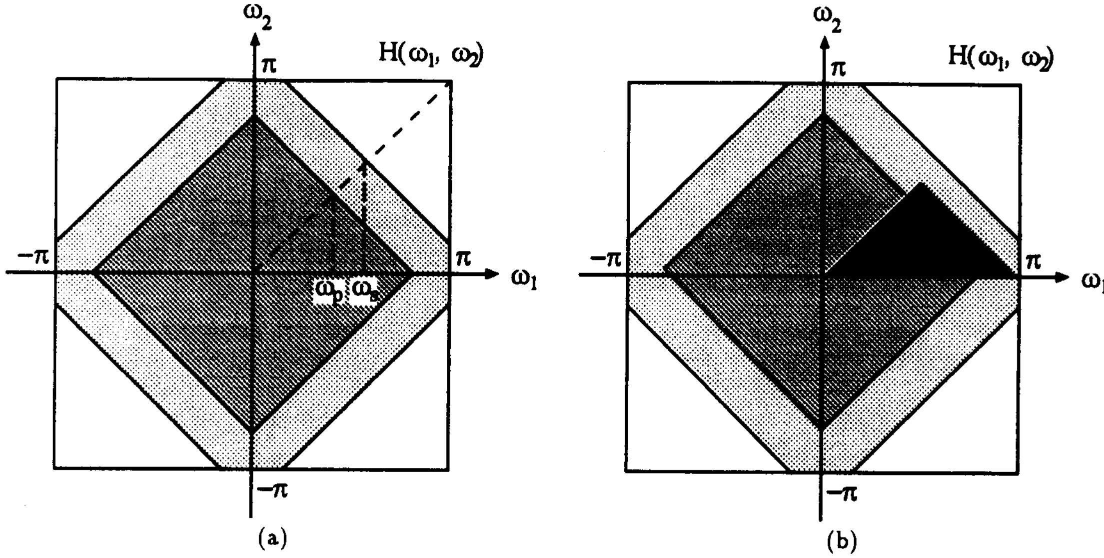

Figure 5: (a) Frequency-response specification of a diamond filter. Shaded region: passband, dotted region: transition band, unshaded region: stopband. (b) The darkly shaded region is the only independent part, because of eightfold symmetry and the half-band nature of the filter.

where $P = (N-1)/2$.

The N_i independent points in the impulse response lie in a wedge-shaped region below the diagonal line $n_1 = n_2$ in the first quadrant of the (n_1, n_2) spatial plane. Thus, the frequency response of a diamond filter can be expressed as [9]

$$\begin{aligned} H(\omega_1,\omega_2) &= 0.5 + \sum_{n_1=1}^{\lfloor (P+1)/2 \rfloor} 2h[2n_1-1,0]\{\cos(2n_1-1)\omega_1 + \cos(2n_1-1)\omega_2\} \\ &+ \sum_{n_1=1}^{\lfloor (P+1)/2 \rfloor} \sum_{n_2=1}^{\lfloor P/2 \rfloor} 4h[2n_1-1,2n_2]\{\cos(2n_1-1)\omega_1 \cos(2n_2)\omega_2 \\ &+ \cos(2n_2)\omega_1 \cos(2n_1-1)\omega_2\}. \end{aligned} \tag{5}$$

Due to the eightfold symmetry and the half-band nature of the filter, the only independent part of the frequency response is a triangular area within the passband, as shown in Figure 5(b). In our design method, N_i samples are placed within this region of the frequency plane. If we take a cross-section of $H(\omega_1, \omega_2)$ along the diagonal line $\omega_1 = \omega_2$, it looks like a 1-D half-band lowpass response. We approximate the passband of this response by a 1-D function $H_p(\omega)$, as used for 1-D half-band lowpass filter design in [7]. The order p of the corresponding Chebyshev polynomial $T_p(x)$ is $(N-1)/2$. The samples are then placed on $(N-1)/2$ lines of slope -1, that pass through the extrema of $H_p(\omega)$. All samples on a particular line have the same value and are evenly spaced. The number of samples on successive lines, as we go away from the origin, is given in Table 2, for filter sizes from 7×7 to 31×31. This range of filter sizes is large enough to cover the needs of most practical applications. The given distribution of samples has been found to work well for various choices of the band-edges. Note that if there is only one sample to be placed on a particular contour, it is placed on the ω_1 axis. Finally, the N_i samples are used to solve for the impulse response coefficients in Equation (5).

The proposed design method produces diamond filters of high quality, with low peak ripple and better passband

Table 2: Distribution of samples for diamond filter design. The last column shows the number of samples placed on $(N-1)/2$ successive contours for designing a filter of size $N \times N$, which has N_i independent coefficients.

N	N_i	Number of samples on successive contours
7	4	1, 2, 1
9	6	1, 1, 2, 2
11	9	1, 1, 2, 3, 2
13	12	1, 1, 2, 3, 3, 2
15	16	1, 1, 2, 3, 3, 4, 2
17	20	1, 1, 2, 3, 3, 4, 4, 2
19	25	1, 1, 2, 3, 3, 4, 4, 4, 3
21	30	1, 1, 2, 3, 3, 3, 4, 4, 5, 4
23	36	1, 1, 2, 3, 3, 3, 4, 4, 5, 6, 4
25	42	1, 1, 2, 3, 3, 4, 4, 4, 5, 6, 6, 5
27	49	1, 1, 2, 3, 3, 4, 4, 4, 5, 6, 6, 6, 5
29	56	1, 1, 2, 3, 3, 4, 4, 4, 5, 6, 6, 6, 7, 5
31	64	1, 1, 2, 3, 3, 4, 4, 4, 5, 6, 6, 6, 7, 7, 6

Table 3: Comparative performance for diamond filter design.

Method	δ_p	δ_s
NDFT	0.0189	0.0184
Frequency Transformation	0.0636	0.0636
Bamberger-Smith	0.1085	0.1084
Chen-Vaidyanathan	0.0292	0.0281

shape as compared to filters produced by other existing design methods. A comparison between these methods is presented in the following example.

Example 2. Consider the design of a diamond filter with the specifications: support size = 9×9, $\omega_p = 0.36\pi$, $\omega_s = 0.64\pi$. Only six of the 81 filter coefficients are independent. The six samples are placed, as depicted on the contour plot in Fig. 6(a), on lines that follow the diamond shape. The diagonal cross-section of the 2-D frequency response is represented by a function $H_p(\omega)$, that has four extrema. Samples are placed on four lines passing through these extrema. The number of samples on these lines are $1, 1, 2, 2$, respectively, as given in Table 2.

For comparison, we now consider three existing methods for designing diamond filters: (i) frequency transformation [8], (ii) the method proposed by Bamberger and Smith [10], and (iii) the method proposed by Chen and Vaidyanathan [11]. We use each of these methods to design a diamond filter with the same specifications as given in Example 2. Their comparative performance is shown in Table 3. For comparison, the frequency response and contour plot of the filter designed by Method (ii) are included in Figure 6(b). In Method (i), a lowpass 1-D filter (of length 9) is transformed to a 2-D diamond filter using a 3×3 transformation. This produces contours which are more circular rather than diamond-shaped. The shape of the contours can be improved by using a higher order transformation, but this also increases the filter size considerably. In this example, if we use a 5×5 trans-

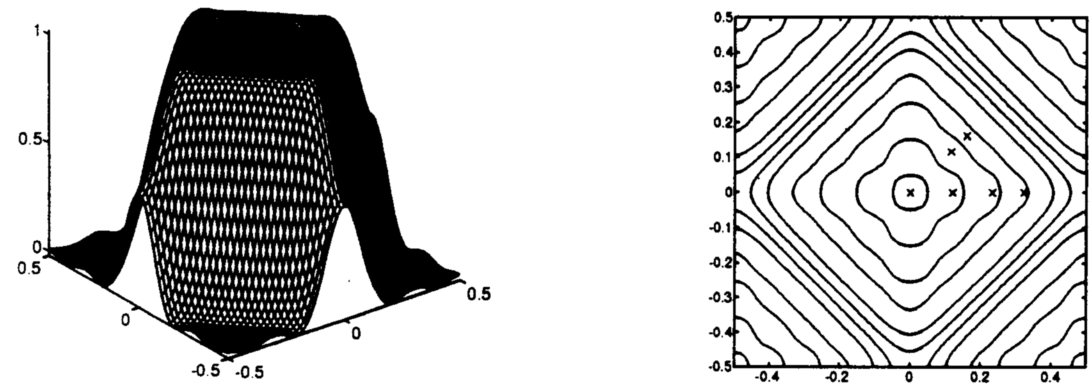

(a)

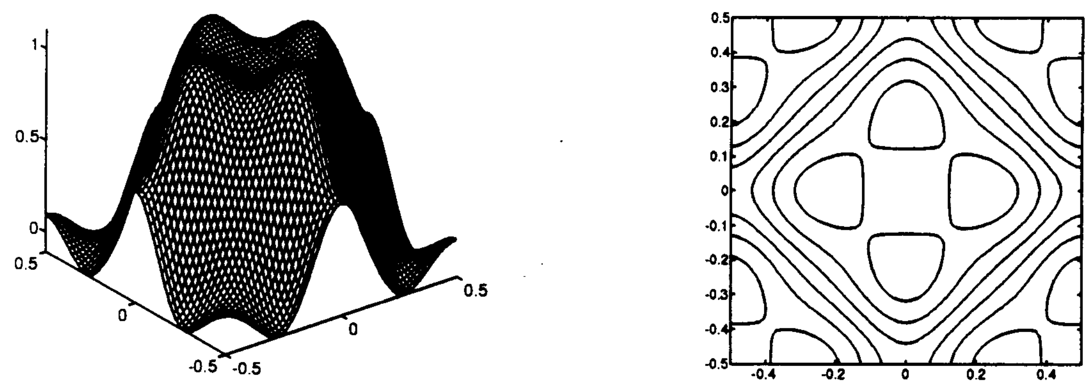

(b)

Figure 6: Frequency response and contour plot for diamond filters of size 9×9 designed by (a) NDFT method, and (b) Bamberger and Smith's method. The sample locations for the NDFT method are denoted by "$\times$" on the corresponding contour plot.

Table 4: PSNR for diamond filters in quincunx downsampling scheme.

Filter design method	PSNR (dB)
NDFT	35.12
Bamberger-Smith	20.70

Table 5: PSNR for square filters in rectangular downsampling scheme.

Filter design method	PSNR (dB)	
	Without codec	With codec
NDFT	29.68	29.05
Separable	24.99	24.83

formation and the same 1-D filter of length 9, then the 2-D filter size becomes 17×17. So this is uneconomical. In Method (ii), a diamond filter is designed by rotating a checkerboard-shaped filter [10] through an angle of 45 degrees. Although the shape of the contours is better than for frequency transformation, the ripple is too large. Method (iii) produces a diamond filter with a good passband shape as well as low peak ripple, comparable to the results obtained by our method. From Table 3, we can see that the NDFT method gives the lowest peak ripple among these methods as well as good contour shapes.

5 APPLICATIONS OF 2-D FILTERS

We now consider applications of 2-D filters as ***prefilters*** prior to downsampling, and as ***postfilters*** for interpolating zero-valued samples after upsampling of images. Square-and diamond-shaped filters are used in schemes for rectangular and quincunx downsampling, respectively.

Example 3. We consider an example application for diamond filters, as prefilters and postfilters in a quincunx downsampling scheme, shown in Figure 7. Such schemes are used to reduce the data rate for digital transmission of HDTV signals. Quincunx downsampling is preferred to orthogonal downsampling because the former does not limit resolution in the horizontal and vertical directions—the human visual system is more sensitive along these directions. We compare the performances of two diamond filters in Example 2, designed by the NDFT method and Bamberger-Smith's method. The LENA image was used. Figure 9 shows the output images. With the input image as reference, we compute the peak signal-to-noise ratio (PSNR) [12] for each output image. A comparison of the PSNR values is given in Table 4. The image produced by using Bamberger-Smith's diamond filter appears to have lower brightness and contrast, and thus, has a lower PSNR.

Example 4. In this example, we evaluate the performance of two square filters designed in Example 1 by the NDFT and separable design methods. These filters are applied in a typical scheme for rectangular downsampling shown in Figure 8. We used the JPEG codec [13] to observe the effect of coding the smaller, downsampled image. The overall bit rate with the codec is 0.5 bits/pixel. This includes the 4:1 reduction due to downsampling. For reference, the input image was also coded using JPEG only (without downsampling) at 0.5 bits/pixel. Although this image is sharper, it exhibits strong block artifacts, visible in the plain regions. Such artifacts are not present in the image produced by the downsampling scheme, due to the smoothing effect of the filters. The PSNR values

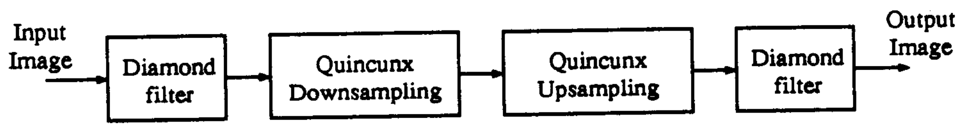

Figure 7: A quincunx downsampling scheme with diamond filters as prefilters and postfilters.

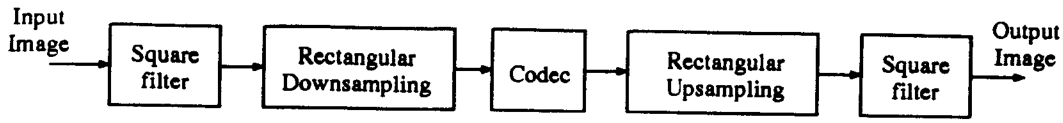

Figure 8: A rectangular downsampling scheme with square filters as prefilters and postfilters.

are given in Table 5. The square filter designed by the NDFT method performs better than the separable square filter in both cases.

6 CONCLUSION

We have developed a nonuniform frequency sampling technique for designing 2-D FIR filters. This method utilizes the freedom of locating samples nonuniformly in the frequency plane to produce nonseparable 2-D filters with good passband shapes and low peak ripples. We have demonstrated the design of square-and diamond-shaped 2-D filters using the proposed method and compared our results with other existing design methods. Note that the proposed filter design method is general, and has been successfully used to design other types of 2-D filters with circular, elliptic, and fan shapes [6]. Earlier nonuniform frequency sampling design methods did not lay down clear guidelines for the choice of sample values and locations. The results are significant owing to the lack of a practical, reliable algorithm to design optimal 2-D filters. We have also investigated the performances of the square-and diamond-shaped filters designed, by applying them as prefilters and postfilters to schemes for rectangular and quincunx downsampling of images, respectively. Considering the general problem of nonuniform frequency sampling, we laid down some specific guidelines regarding the choice of the sample values and locations, which were lacking in earlier techniques. These guidelines can serve as a basis for the design of more complex 2-D filters.

7 ACKNOWLEDGEMENTS

This research was supported in part by an internship provided to the first author with the Signal Processing Group, Communication Systems Research Laboratory, Tektronix, Inc., and in part by a University of California MICRO grant with matching funds from Tektronix, Inc., Rockwell International Corporation, and Digital Instruments, Inc. The authors would like to thank Drs. Ganesh Rajan and Ajay Luthra for their helpful discussions.

8 REFERENCES

[1] S.K. Mitra, S. Chakrabarti, and E. Abreu, "Nonuniform discrete Fourier transform and its applications in signal processing," in *Proc. EUSIPCO '92, Sixth European Signal Processing Conference*, vol. 2, (Brussels, Belgium), pp. 909–912, August 1992.

[2] J.E. Diamessis, C.W. Therrien, and W.J. Rozwood, "Design of 2-D FIR filters with nonuniform frequency samples," in *Proc. IEEE Int. Conf. on Acoust., Speech, Signal Processing*, vol. 3, (Dallas, TX), pp. 1665–1668, April 1987.

[3] E. Angelides, "A novel method for modeling 2-D FIR digital filters in frequency domain with nonuniform

(a) (b)

Figure 9: Images produced by quincunx downsampling scheme, with diamond filters designed by: (a) NDFT method. (b) Bamberger-Smith's method.

samples," *IEEE Trans. Circuits Syst. II: Analog and Digital Signal Processing*, vol. 41, pp. 482–486, July 1994.

[4] W.J. Rozwood, C.W. Therrien, and J.S. Lim, "Design of 2-D FIR filters by nonuniform frequency sampling," *IEEE Trans. Acoust., Speech, Signal Processing*, vol. ASSP-39. pp. 2508–2514, November 1991.

[5] A. Zakhor and G. Alvstad, "Two-dimensional polynomial interpolation from nonuniform samples," *IEEE Trans. Acoust., Speech, Signal Processing*, vol. ASSP-40, pp. 169–180, January 1992.

[6] S. Bagchi, *The Nonuniform Discrete Fourier Transform and its Applications in Signal Processing.* Ph.D dissertation, University of California at Santa Barbara, 1994.

[7] M. Lightstone, S.K. Mitra, I.-S. Lin, S. Bagchi, P. Jarske, and Y. Neuvo, "Efficient frequency-sampling design of one-and two-dimensional FIR filters using structural subband decomposition," *IEEE Trans. Circuits Syst. II: Analog and Digital Signal Processing*, vol. 41, pp. 189–201, March 1994.

[8] J.S. Lim, *Two-Dimensional Signal and Image Processing.* Englewood Cliffs, N.J.: Prentice-Hall, 1990.

[9] T. Yoshida, A. Nishihara, and N. Fujii, "A design method of 2-D maximally flat diamond-shaped half-band FIR filters," *Trans. IEICE (The Institute of Electronics, Information and Communication Engineers)*, vol. E 73, pp. 901–907, June 1990.

[10] R.H. Bamberger and M.J.T. Smith, "A filter bank for the directional decomposition of images: Theory and design," *IEEE Trans. Signal Processing*, vol. 40, pp. 882–893, April 1992.

[11] T. Chen and P.P. Vaidyanathan, "Multidimensional multirate filters and filter banks derived from one-dimensional filters," *IEEE Trans. Signal Processing*, vol. 41, pp. 1749–1765, May 1993.

[12] W.K. Pratt, *Digital Image Processing.* New York: John Wiley & Sons, 1991.

[13] A. Leger, T. Omachi, and G.K. Wallace, "JPEG still picture compression algorithm," *Optical Engineering*, vol. 30, pp. 947–954, July 1991.